



## **Spin Torque Nano Oscillators as Potential Terahertz (THz) Communications Devices**

**by Alma E. Wickenden, Chris Fazi, Ben Huebschman, Roger Kaul,  
Andrew C. Perrella, William H. Rippard, and Matthew R. Pufall**

**ARL-TR-4807**

**April 2009**

## **NOTICES**

### **Disclaimers**

The findings in this report are not to be construed as an official Department of the Army position unless so designated by other authorized documents.

Citation of manufacturer's or trade names does not constitute an official endorsement or approval of the use thereof.

Destroy this report when it is no longer needed. Do not return it to the originator.

# **Army Research Laboratory**

Adelphi, MD 20783-1197

---

---

**ARL-TR-4807**

**April 2009**

---

## **Spin Torque Nano Oscillators as Potential Terahertz (THz) Communications Devices**

**Alma E. Wickenden, Chris Fazi, Ben Huebschman,  
Roger Kaul, and Andrew C. Perrella  
Sensors and Electron Devices Directorate, ARL**

**William H. Rippard and Matthew R. Pufall,  
National Institute of Standards & Technology, Boulder, CO**

REPORT DOCUMENTATION PAGE			Form Approved OMB No. 0704-0188		
Public reporting burden for this collection of information is estimated to average 1 hour per response, including the time for reviewing instructions, searching existing data sources, gathering and maintaining the data needed, and completing and reviewing the collection information. Send comments regarding this burden estimate or any other aspect of this collection of information, including suggestions for reducing the burden, to Department of Defense, Washington Headquarters Services, Directorate for Information Operations and Reports (0704-0188), 1215 Jefferson Davis Highway, Suite 1204, Arlington, VA 22202-4302. Respondents should be aware that notwithstanding any other provision of law, no person shall be subject to any penalty for failing to comply with a collection of information if it does not display a currently valid OMB control number. <b>PLEASE DO NOT RETURN YOUR FORM TO THE ABOVE ADDRESS.</b>					
1. REPORT DATE (DD-MM-YYYY) April 2009		2. REPORT TYPE Final		3. DATES COVERED (From - To) FY 07–FY 08	
4. TITLE AND SUBTITLE Spin Torque Nano Oscillators as Potential Terahertz (THz) Communications Devices			5a. CONTRACT NUMBER		
			5b. GRANT NUMBER		
			5c. PROGRAM ELEMENT NUMBER		
6. AUTHOR(S) Alma E. Wickenden, Chris Fazi, Ben Huebschman, Roger Kaul, Andrew C. Perrella, William H. Rippard, and Matthew R. Pufall			5d. PROJECT NUMBER		
			5e. TASK NUMBER		
			5f. WORK UNIT NUMBER		
7. PERFORMING ORGANIZATION NAME(S) AND ADDRESS(ES) U.S. Army Research Laboratory ATTN: AMSRD-ARL-SE-RL 2800 Powder Mill Road Adelphi, MD 20783-1197			8. PERFORMING ORGANIZATION REPORT NUMBER ARL-TR-4807		
9. SPONSORING/MONITORING AGENCY NAME(S) AND ADDRESS(ES)			10. SPONSOR/MONITOR'S ACRONYM(S)		
			11. SPONSOR/MONITOR'S REPORT NUMBER(S)		
12. DISTRIBUTION/AVAILABILITY STATEMENT Approved for public release; distribution unlimited.					
13. SUPPLEMENTARY NOTES					
14. ABSTRACT In this report, we describe the complex impedance of spin torque nano oscillator (STNO) devices. We determined that the STNO is a nonreactive, real-resistance device with single-valued resistance in the broadband frequency range of 500 MHz to 10 GHz (the limit of our test conditions), and that STNOs do not require an external circuit or conjugate matching to operate in a transmitter configuration. We report the first demonstration of the low-power (250 pW), high-frequency (9 GHz) microwave output from an antenna-coupled discrete 50 nm diameter magnetic STNO radiating through air over a distance of 1 m. Amplitude and frequency modulation of the output radiation was used to transmit information from the STNO through microwave antennas. In addition to our identification of the STNO as a highly unusual broadband component that is frequency agile over at least four octaves of frequency without conjugate matching, the STNO is inherently radiation hard with an extremely low operating voltage (<0.25 V) compared to solid-state electronic devices including field-effect transistors (FETs), impact ionization avalanche transit time (IMPATT) diodes, and Gunn diodes. The present results establish the viability of using this class of nanoelectronic devices for frequency-agile communications applications at high frequencies.					
15. SUBJECT TERMS Spin torque nano-oscillator, impedance, nanoelectronics, nanomagnetism, spin dynamics					
16. SECURITY CLASSIFICATION OF:			17. LIMITATION OF ABSTRACT UU	18. NUMBER OF PAGES 20	19a. NAME OF RESPONSIBLE PERSON Alma E. Wickenden
a. REPORT Unclassified	b. ABSTRACT Unclassified	c. THIS PAGE Unclassified			19b. TELEPHONE NUMBER (Include area code) (301) 394-0094

---

## Contents

---

<b>List of Figures</b>	<b>iv</b>
<b>Acknowledgments</b>	<b>v</b>
<b>1. Objective</b>	<b>1</b>
<b>2. Approach</b>	<b>1</b>
<b>3. Results</b>	<b>4</b>
<b>4. Conclusions</b>	<b>7</b>
<b>5. References</b>	<b>8</b>
<b>6. Transitions</b>	<b>9</b>
<b>List of Symbols, Abbreviations, and Acronyms</b>	<b>10</b>
<b>Distribution List</b>	<b>11</b>

---

## List of Figures

---

Figure 1. STNO device geometry. ....	2
Figure 2. Frequency modulation of STNO; in this device geometry, frequency decreases with increasing applied drive current. ....	4
Figure 3. Configuration of STNO (left) and the experiment schematic (right), which illustrates both the configuration of the RF signal collected through coaxial cable (a) and the antenna configuration (b) for experiments described in the text. ....	4
Figure 4. A 1-port s-parameter analysis of an STNO device over a 0.5–10 GHz frequency range, with probe and cable impedance de-embedded from circuit analysis: (a) short circuit, (b) open circuit, (c) STNO with no applied drive current or magnetic field, and (d) active STNO with $-7.5$ mA drive current and $+0.26$ T magnetic field applied. All tests performed at various drive currents and applied field strengths were found to be equivalent to (d). ....	5
Figure 5. Frequency modulated STNO signals broadcast through (a) air and (b) coaxial cable, using the experimental configuration in figure 3. Typical spectral linewidth for this device is observed in (a) for data collected in single sweep mode. Characteristic phase noise for the device is observed in (b) for data collected in maximum hold mode. ....	6

---

## **Acknowledgments**

---

We would like to acknowledge beneficial discussions with D. C. Judy and J.X.Z. Qiu on microwave measurements, and the helpful assistance of R. Ralph and A. Roy with experimental fixturing and M. L. Chin with the automation of data collection.

INTENTIONALLY LEFT BLANK.

---

## 1. Objective

---

The objective of this research is to investigate the feasibility of sub-100 nm spin torque nano oscillator (STNO) devices for radiating energy through space. We describe the complex impedance of the STNO from 0.5–10 GHz, and report what we believe to be the first demonstration of the low-power (250 pW), high-frequency (9 GHz) microwave output from an antenna-coupled, discrete, 50-nm diameter magnetic oscillator radiating through air over a distance of 1 m. Amplitude and frequency modulation of the output radiation has been used to transmit information from the STNO through microwave antennas.

---

## 2. Approach

---

The need for compact, high-frequency wireless communications for microwave data links and remote sensing is envisioned for future Army applications. Although limited at present by low efficiency operation, magnetic STNOs are the only radio frequency (RF) technology operating at  $<0.25$  V and are a promising new class of devices that hold potential as low-voltage, room-temperature, frequency-agile, nanoscale radiative sources that can be fabricated on-chip. The frequency response of STNOs can be tuned as a function of drive current or applied magnetic field, with theoretically predicted oscillation frequencies from MHz to hundreds of GHz, and possibly up to 1 THz in devices approaching 5 nm in diameter (1). STNO devices operating in the 1–40 GHz range have been the subject of active investigation for several years (2–4) with spectrum analysis of the device response reported using a point contact configuration with a bias tee and microwave coaxial cable. However, to date there has been no demonstration of an STNO's ability to radiate energy through space, and very little is understood about the microwave impedance of a low-power (pW–nW) STNO device as a function of frequency. Impedance matching of an RF device in a circuit is typically required to maximize power transfer. An understanding of the impedance characteristics of the STNO is desired to minimize insertion loss, reflection, and attenuation, thus serving to increase the transmitted power of the very weak STNO signal and resultant  $10^{-6}$  efficiency (defined as RF power out/DC power in) observed in coaxial experiments to date. It is also necessary from a systems standpoint to understand the frequency dependence of the impedance to enable controlled frequency modulation of the transmitted signal.

The operating principle of the STNO device, which is illustrated schematically in figure 1, is that a DC current passing through a thick (fixed) magnetic layer polarizes the electron spins in the current. These polarized spins then flow through a thin (free) magnetic layer and produce enough spin torque to cancel out the intrinsic damping torque of the thin magnetic film (5). As a

result, the electron spins within the free magnetic film are able to precess about an applied magnetic field.

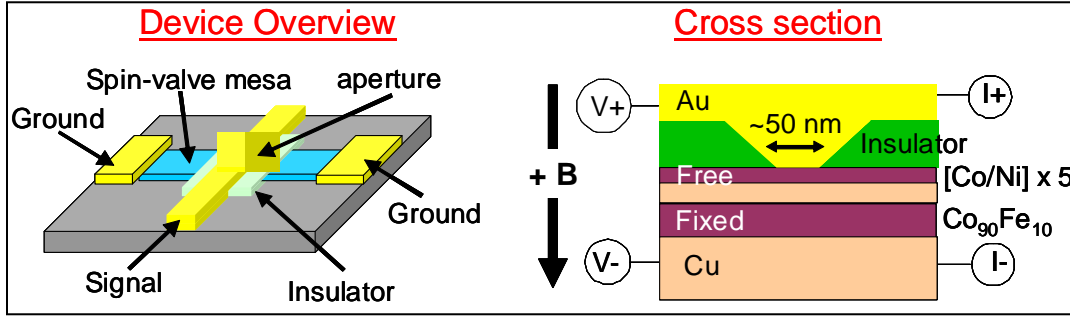


Figure 1. STNO device geometry.

The unpolarized electron current passes through the thick magnetic layer with magnetization  $\mathbf{m}_f$ . The fixed magnetic layer acts as a polarizer and the electrons that exit the film are now polarized with spin,  $\mathbf{S}_i$ . In the STNO device, these electrons then pass through a nonmagnetic metal spacer layer. As long as the spin-dependent mean free path of the spacer layer is much larger than the spacer thickness,  $\mathbf{S}_i$  will be preserved. As this polarized current passes through the thinner free layer with arbitrary magnetization  $\mathbf{M}$ , it will once again be polarized with resultant spin  $\mathbf{S}_f$ . Therefore, the torque exerted on the spin of the electron will be equal to the difference of these spins,  $\mathbf{T}_S = \mathbf{S}_f - \mathbf{S}_i$ . Newton's third law dictates that the torque exerted by the spin on the free layer ( $\mathbf{T}_M$ ) must be equal and opposite,  $\mathbf{T}_M = -\mathbf{T}_S$ . It should be noted that reversing the current direction causes the electrons that are reflected from the fixed layer to deliver their spin to the free layer. These reflected electrons will have an opposite spin,  $-\mathbf{S}_i$ , relative to those which are polarized by  $\mathbf{m}_f$ . Hence, reversing the current direction reverses the torque  $\mathbf{T}_M$ . With such a torque term and with high enough current densities (typically above  $10^7$  A/cm<sup>2</sup>), the alignment (and anti-alignment) of  $\mathbf{M}$  with  $\mathbf{m}_f$  is possible in magnetic nanostructures with two stable configurations.

This spin transfer effect has been demonstrated, first by Myers et al. (6) and verified by others (7, 8). The high current densities required are typically achieved by reducing the size of the device to below 100 nm. While the ability to switch a magnetic layer with a DC current is encouraging for magnetic memory based applications, the magnetic dynamics application based on this torque term is of interest to the present work. The dynamics of the free layer can be written in terms of the Landau-Lifshitz-Gilbert equation, as shown in equation 1 (1):

$$\frac{d\vec{M}}{d\tau} = \underbrace{-|\gamma|\mu_0 \vec{M} \times \vec{H}_{\text{eff}}}_{\text{precession}} - \underbrace{\frac{2}{M_s^2} T_2 \vec{M} \times (\vec{M} \times \vec{H}_{\text{eff}})}_{\text{LL damping}} + \underbrace{\beta(x) \vec{M} \times (\vec{M} \times \hat{m}_f)}_{\text{spin torque}} \quad (1)$$

Here  $H_{\text{eff}}$  is the effective magnetic field comprised of the applied magnetic field, the demagnetizing field, and the exchange field. The terms  $\gamma$ ,  $\mu_0$ ,  $M_s$ ,  $T$ , and  $\beta$  are the gyromagnetic ratio, permeability of free space, saturation magnetization of the free layer, the lateral relaxation time, and the spin torque driving term, respectively. The spin torque term can cancel the Landau-Lifshitz (LL) damping term, resulting in a magnetic moment that will freely rotate about an applied magnetic field. These precessions have been demonstrated at frequencies up to 40 GHz (2) and are currently limited only by measurement equipment constraints. Modulation of the STNO oscillation frequency has been demonstrated in contact mode measurements with modulation frequencies up to half the carrier frequency (8).

The STNO devices used in the present research were fabricated at National Institute of Standards and Technology (NIST), Boulder, CO. They consist of a 50-nm diameter electrical contact made to the top of a 10 x 20  $\mu\text{m}$  spin-valve mesa. The spin valve comprises substrate/tantalum (Ta) (3 nm)/copper (Cu) (15 nm)/  $\text{Co}_{90}\text{Fe}_{10}$  (20 nm)/Cu (4.5 nm)/ {Co(0.3nm)/Ni(0.5nm)} $\times$ 5/gold (Au) (3 nm). In this structure, precessional motion is induced in the cobalt (Co)/nickel (Ni) multilayer (“free layer”), and the cobalt-iron (CoFe) layer acts as the “fixed” layer due to its larger thickness and saturation magnetization. The devices are DC current biased in a current perpendicular to the plane geometry, so that precessional motion of the free layer induces a microwave voltage across the device through the giant magnetoresistance (GMR) effect, resulting in emission at the precession frequency.

For the purposes of detailed characterization, our measurements focused on device operation near 10 GHz to allow for the use of a greater range of available instrumentation for measurement of the radiated signal. We contacted the STNO devices with a ground-signal-ground (GSG) RF probe and microwave coaxial cable, and positioned the fixture between the poles of an electromagnet capable of producing magnetic fields of 0.2–0.4 T. We oriented the device axis parallel to the applied magnetic field to maximize oscillation response (9). The drive current was applied to the STNO device through a 50 GHz bandwidth, 7 ps risetime bias tee using an AC/DC current source with the voltage monitored using a nanovoltmeter. We used a 26 dB gain low-noise amplifier (LNA) to overcome the 50-GHz spectrum analyzer high noise input. We selected operating conditions for drive current and applied magnetic field for each device tested to maximize signal output power and avoid conditions where broad, bimodal oscillation behavior was observed, as shown in figure 2. We investigated the S-parameters of the STNO device in a 1-port configuration using a network analyzer. For transmission of the STNO output through air, the STNO output was fed through a length of coaxial cable directly into a WR90 waveguide horn antenna having a ~9–11 GHz, 20 dB gain. We used a matching antenna to receive the signal, inserting the LNA into the circuit after the receive antenna. Figure 3 illustrates the experimental configurations.

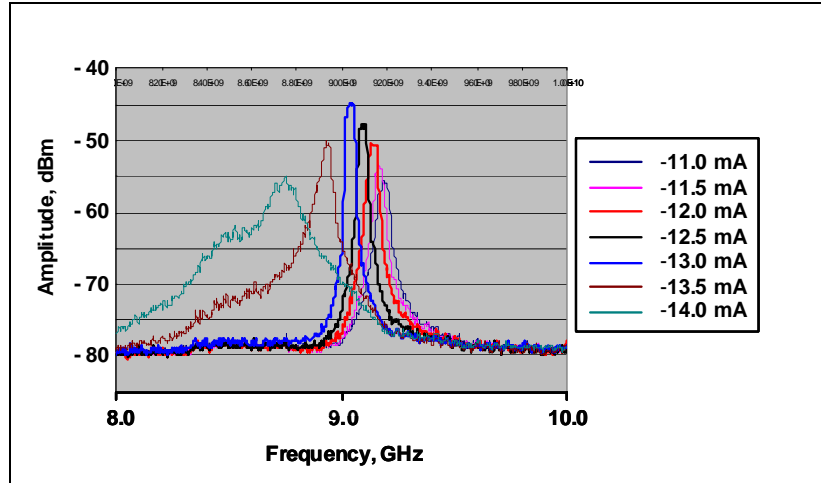


Figure 2. Frequency modulation of STNO; in this device geometry, frequency decreases with increasing applied drive current.

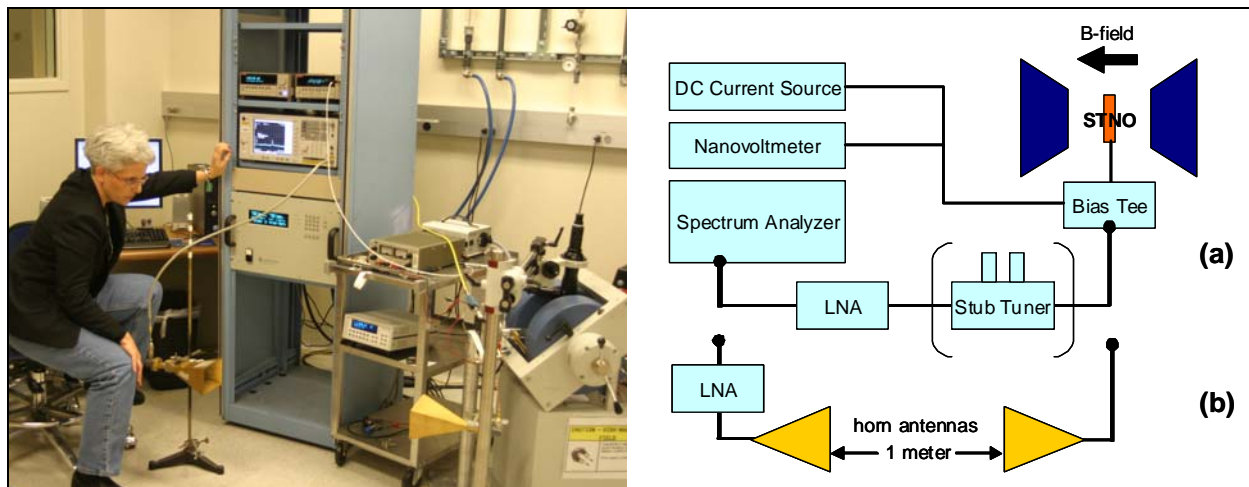


Figure 3. Configuration of STNO (left) and the experiment schematic (right), which illustrates both the configuration of the RF signal collected through coaxial cable (a) and the antenna configuration (b) for experiments described in the text.

### 3. Results

Our efforts to improve the impedance matching of the circuit containing the STNO device by using a double stub tuner in the coaxial experimental configuration shown in figure 3a were unsuccessful. We observed a periodic reduction in signal intensity upon tuning through  $\lambda/2$  intervals, but no enhancement of the signal, suggesting either significant phase noise or possibly very low impedance.

We performed scattering (s-) parameter measurements using a network analyzer that was calibrated to the end of its cables using a commercially available calibration kit. Since the STNO sample lacked the complete set of calibration standards typically required to perform a full 1-port characterization of the GSG probe, we determined the reflection coefficient of the STNO device by measuring the components connected to the GSG probe and modeling the probe as a transmission line. The s-parameters for the coaxial transmission line to the probe were measured independently on the network analyzer, and the measurement was recorded and saved. The s-parameters of the probe, coaxial transmission line, and the STNO device were measured at bias conditions of  $-7.5$  mA and  $-8.0$  mA, at magnetic field strengths of  $+0.26$  T,  $+0.27$  T, and  $+0.28$  T for each bias condition, representing optimized operating conditions for this device. To determine the reflection coefficient of the STNO, we de-embedded the measured transmission line s-parameters from the sample; the characteristic Smith chart plots are shown in figure 4.

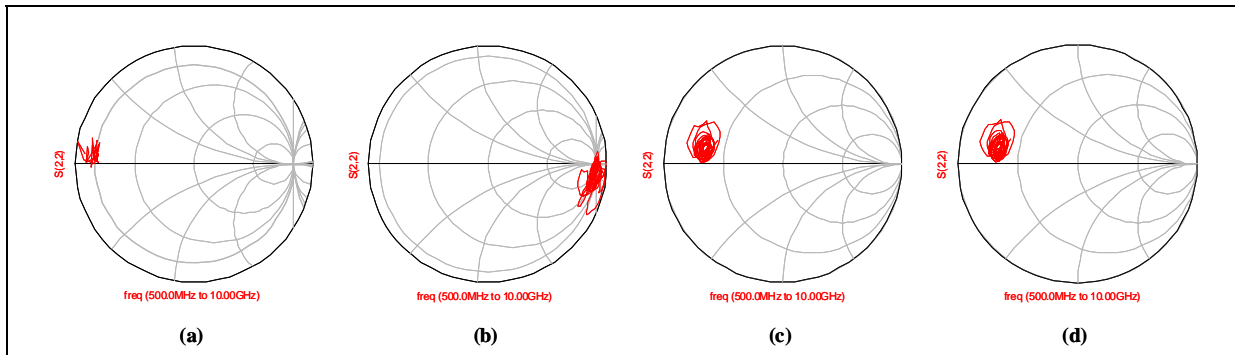


Figure 4. A 1-port s-parameter analysis of an STNO device over a 0.5–10 GHz frequency range, with probe and cable impedance de-embedded from circuit analysis: (a) short circuit, (b) open circuit, (c) STNO with no applied drive current or magnetic field, and (d) active STNO with  $-7.5$  mA drive current and  $+0.26$  T magnetic field applied. All tests performed at various drive currents and applied field strengths were found to be equivalent to (d).

We determined the length of the equivalent transmission line model for the probe and device by finding the length that, when de-embedded from the measured data from the probe tips resting on a gold strip, produced an impedance consistent with what would be predicted for a short circuit. We confirmed this by de-embedding the same length transmission line from data measured when the probes were resting on the insulating substrate. This adjustment produced an impedance value consistent with what would be predicted from an open circuit. Modeling the GSG probe as a transmission line produced reasonably correct impedances up to 10 GHz for a short and open circuit. Above 10 GHz, the technique developed to determine the s-parameters proved to be unreliable; therefore, we did not analyze any data beyond this frequency.

We applied this procedure to the s-parameters measured from the STNO, which we determined produced a purely resistive impedance from 500 MHz to 10 GHz, the limit of the analytical method applied. We determined the RF impedance to be 12.5 Ohms independent of applied drive current or magnetic field, which is very close to the measured DC resistance of 11.25 Ohms. This finding is significant, revealing that *the STNO represents a highly unusual*

*broadband component that is frequency agile over at least four octaves of frequency, with no need for any conjugate matching as required for field-effect transistors (FETs), impact ionization avalanche transit time (IMPATT) diodes, Gunn diodes, and other solid-state electronic devices.*

We then demonstrated amplitude- and frequency-modulated 9-GHz radiation from a discrete STNO device coupled to a horn antenna through air over a 1-m distance, with the STNO device configured as in figure 3b. The STNO device was biased at optimized operating conditions using a +0.30 T applied magnetic field and varying the bias current between  $-12$  to  $-13$  mA to modulate the output signal frequency in a quasi-DC fashion. Figure 5a shows the frequency-modulated signal captured by the spectrum analyzer in a single-sweep mode. We observed the amplitude modulation by keying the STNO bias on and off in the Morse code letter “V” and observing the signal recovery on the spectrum analyzer. Figure 5b shows the frequency modulated data for the same device using the coaxial transmission configuration of figure 3a (without the stub tuner). In this case, we collected the data in maximum hold mode to illustrate the characteristic envelope of variation in the STNO frequency output (i.e., jitter) over time. We observed a signal bandwidth as high as 300 MHz in both experimental configurations for data collected over a period of 5 min or longer. We attributed the poor frequency stability of these devices to the use of a novel device geometry. Similar devices fabricated from different materials have shown spectral linewidths as small as 2 MHz (2), and improved spectral linewidths have been observed in more recently grown structures where the film roughness of the Co/Ni free layers has been reduced. Phase locking of STNOs has also been demonstrated, in which tenfold enhancement in power spectral density has been observed (10).

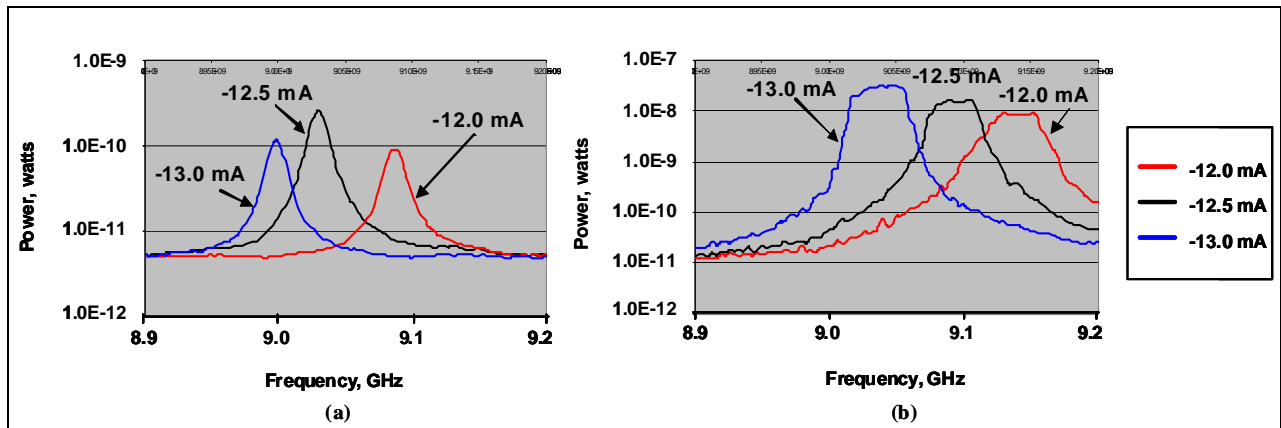


Figure 5. Frequency modulated STNO signals broadcast through (a) air and (b) coaxial cable, using the experimental configuration in figure 3. Typical spectral linewidth for this device is observed in (a) for data collected in single sweep mode. Characteristic phase noise for the device is observed in (b) for data collected in maximum hold mode.

The transmission efficiency (figure 5) decreases by two orders of magnitude in the antenna-coupled transmission, where a nominally 250-pW signal is observed compared to the nominal 160-nW signal seen in the coaxial transmission. This is consistent with the expected free space

geometric losses. We attribute the frequency offset observed in the data sets of figure 5, which were collected from the same device under the same conditions of bias and applied magnetic field, either to different loading conditions or to the effects of slight geometrical differences in the experimental configuration between the two measurements.

---

## **4. Conclusions**

---

We have demonstrated the first frequency- and amplitude-modulated transmission of the signal from a discrete, antenna-coupled STNO device through air over a distance of 1 m, establishing the viability of using this class of nanoelectronic devices for frequency-agile communications applications at high frequencies. We determined that the STNO is a nonreactive, real-resistance device, operating in the broadband range from 500 MHz to 10 GHz (the limit of our test conditions), and that STNOs do not require an external circuit nor conjugate matching to operate in a transmitter configuration. The STNO represents a highly unusual broadband component that is frequency agile over at least four octaves of frequency without conjugate matching and is inherently radiation hard with extremely low operating voltage ( $<0.25$  V). These findings suggest that the STNO may hold potential advantages over FETs, IMPATT diodes, Gunn diodes, and other solid-state electronic devices in select applications.

---

## 5. References

---

1. Hofer, M. A.; Ablowitz, M. J.; Ilan, B.; Pufall, M. R.; Silva, T. J. *Phys. Rev. Lett.* **2005**, *95*, 267206.
2. Rippard, W. H.; Pufall, M. R.; Kaka, S.; Russek, S. E.; Silva, T. J. *Phys. Rev. Lett.* **2004**, *92*, 027201.
3. Kiselev, S. I.; Sankey, J. C.; Kirvorotov, I. N.; Emley, N. C.; Schoelkopf, R. J.; Buhrman, R. A.; Ralph, D. C. *Nature* **2003**, *425* (6956), 380–383.
4. Covington, M.; AlHajDarwish, M.; Ding, Y.; Rebei, A.; Parker, G. J.; Gokemeijer, N.; Seigler, M. A. *J. Magnetism & Magnetic Matls.* **2005**, *287*, 325–332.
5. For a thorough review of spin transfer torques, see Ralph, D. C.; Stiles, M. D. *J. Magnetism & Magnetic Matls.* **2008**, *320*, 1190–1216 (2008), and references therein.
6. Meyers, E. B.; Ralph, D. C.; Katine, J. A.; Louie, R. N.; Buhrman, R. A. *Science* **2000**, *285*, 867–870.
7. Katine, J. A.; Albert, F. J.; Buhrman, R. A.; Meyers, E. B.; Ralph, D. C.; *Phys. Rev. Lett.* **2000**, *84*, 3149–3152
8. Rippard, W. H.; Pufall, M. R.; Silva, T. J. *Appl. Phys. Lett.* **2003**, *82*, 1260–1262.
9. Rippard, W. H.; Pufall, M. R.; Kaka, S.; Silva, T. J.; Russek, S. E. *Phys. Rev. B* **2004**, *70* 100406.
10. Kaka, S.; Pufall, M. R.; Rippard, W. H.; Silva, T. J.; Russek, S. E.; Katine, J. A. *Nature Letters* **2005**, *437*, 389.

---

## 6. Transitions

---

We are currently preparing a manuscript for intended submission to *Applied Physics Letters* or *Nature Physics*. Discussions are underway investigating potential collaborative research on this topic with the Tank and Automotive Research, Development and Engineering Center (TARDEC) and the Communications-Electronics Research Development and Engineering Center (CERDEC), who have expressed significant interest in these research findings.

---

## List of Symbols, Abbreviations, and Acronyms

---

Au	gold
CERDEC	Communications-Electronics Research Development and Engineering Center
Co	cobalt
Cu	copper
Fe	iron
FETs	field-effect transistors
GMR	giant magnetoresistance
GSG	ground-signal-ground
IMPATT	impact ionization avalanche transit time
LL	Landau-Lifshitz
LNA	low-noise amplifier
Ni	nickel
RF	radio frequency
STNO	spin torque nano oscillator
Ta	tantalum
TARDEC	Tank and Automotive Research, Development and Engineering Center

<u>No. of Copies</u>	<u>Organization</u>
1 (PDF only)	DEFENSE TECHNICAL INFORMATION CTR DTIC OCA 8725 JOHN J KINGMAN RD STE 0944 FORT BELVOIR VA 22060-6218
1 CD	DIRECTOR US ARMY RESEARCH LAB IMNE ALC HRR 2800 POWDER MILL RD ADELPHI MD 20783-1197
1 CD	DIRECTOR US ARMY RESEARCH LAB AMSRD ARL CI OK TL 2800 POWDER MILL RD ADELPHI MD 20783-1197
1 CD	DIRECTOR US ARMY RESEARCH LAB AMSRD ARL CI OK PE 2800 POWDER MILL RD ADELPHI MD 20783-1197
1 HC	US ARMY TARDEC/RDECOM AMSRD TAR/MS 263 DR GRANT GERHART 6501 E 11 MILE RD WARREN MI 48397-5000
1 HC	US ARMY TARDEC/RDECOM AMSRD TAR R/MS 263 DR ELENA BANKOWSKI 6501 E 11 MILE ROAD WARREN MI 48397-5000
2 HCs	NATIONAL INSTITUTE OF STANDARDS & TECHNOLOGY ELECTROMAGNETICS DIVISION DR. WILLIAM RIPPARD DR. MATTHEW PUFALL 325 BROADWAY BOULDER CO 80305-3328

<u>No. of Copies</u>	<u>Organization</u>
1 HC	US ARMY TARDEC/RDECOM AMSRD TAR R MS 263 DR THOMAS J MEITZLER 6501 E 11 MILE ROAD WARREN MI 48397-5000
1 HC	US ARMY RESEARCH LABORATORY AMSRD ARL SE RL DR BRETT PIEKARSKI 2800 POWDER MILL ROAD ADELPHI MD 20783
1 HC	US ARMY RESEARCH LABORATORY AMSRD ARL SE R DR PAUL AMIRTHARAJ 2800 POWDER MILL ROAD ADELPHI MD 20783
5 HCs	US ARMY RESEARCH LABORATORY DIR SEDD AMSRD ARL SE DR JOHN PELLEGRINO AMSRD ARL SE RE DR. CHRISTIAN FAZI MR. BENJAMIN HUEBSCHMAN DR. ROGER KAUL AMSRD ARL SE RL DR. ALMA WICKENDEN 2800 POWDER MILL ROAD ADELPHI MD 20783
1 HC	OAKLAND UNIVERSITY PROF ANDREI N SLAVIN CHAIR DEPARTMENT OF PHYSICS 190 SCIENCE & ENGINEERING BLDG ROCHESTER MICHIGAN 48309
<u>ABERDEEN PROVING GROUND</u>	
1 CD	DIR USARL AMSRD ARL CI OK TP (BLDG 4600)
TOTAL: 18 (1 ELEC, 4 CDS, 13 HCS)	

INTENTIONALLY LEFT BLANK.